



This is a repository copy of *Ultrafast control of strong light-matter coupling*.

White Rose Research Online URL for this paper:
<http://eprints.whiterose.ac.uk/131139/>

Version: Published Version

Article:

Lange, C., Cancellieri, E., Panna, D. et al. (6 more authors) (2018) Ultrafast control of strong light-matter coupling. *New Journal of Physics*, 20 (1). 013032. ISSN 1367-2630

<https://doi.org/10.1088/1367-2630/aa9fd0>

© 2018 The Author(s). Published by IOP Publishing Ltd on behalf of Deutsche Physikalische Gesellschaft. Original content from this work may be used under the terms of the Creative Commons Attribution 3.0 licence. Any further distribution of this work must maintain attribution to the author(s) and the title of the work, journal citation and DOI. (<http://creativecommons.org/licenses/by/3.0>)

Reuse

This article is distributed under the terms of the Creative Commons Attribution (CC BY) licence. This licence allows you to distribute, remix, tweak, and build upon the work, even commercially, as long as you credit the authors for the original work. More information and the full terms of the licence here:
<https://creativecommons.org/licenses/>

Takedown

If you consider content in White Rose Research Online to be in breach of UK law, please notify us by emailing eprints@whiterose.ac.uk including the URL of the record and the reason for the withdrawal request.



eprints@whiterose.ac.uk
<https://eprints.whiterose.ac.uk/>

PAPER • OPEN ACCESS

Ultrafast control of strong light–matter coupling

To cite this article: Christoph Lange *et al* 2018 *New J. Phys.* **20** 013032

View the [article online](#) for updates and enhancements.



PAPER

Ultrafast control of strong light–matter coupling

Christoph Lange¹, Emiliano Cancellieri², Dmitry Panna³, David M Whittaker², Mark Steger⁴, David W Snoke⁴, Loren N Pfeiffer⁵, Kenneth W West⁵ and Alex Hayat^{3,6}

¹ Department of Physics, University of Regensburg, D-93040 Regensburg, Germany

² Department of Physics and Astronomy, University of Sheffield, Sheffield S3 7RH, United Kingdom

³ Department of Electrical Engineering, Technion, Haifa 32000, Israel

⁴ Department of Physics and Astronomy, University of Pittsburgh, Pittsburgh, PA 15260, United States of America

⁵ Department of Electrical Engineering, Princeton University, Princeton, NJ 08544, United States of America

⁶ Author to whom any correspondence should be addressed.

E-mail: alex.hayat@ee.technion.ac.il

OPEN ACCESS

RECEIVED

24 August 2017

REVISED

17 November 2017

ACCEPTED FOR PUBLICATION

7 December 2017

PUBLISHED

22 January 2018

Original content from this work may be used under the terms of the [Creative Commons Attribution 3.0 licence](https://creativecommons.org/licenses/by/4.0/).

Any further distribution of this work must maintain attribution to the author(s) and the title of the work, journal citation and DOI.



Keywords: strong light–matter coupling, dynamic Stark effect, exciton–polaritons, ultrafast control

Supplementary material for this article is available [online](#)

Abstract

We dynamically modulate strong light–matter coupling in a GaAs/AlGaAs microcavity using intense ultrashort laser pulses tuned below the interband exciton energy, which induce a transient Stark shift of the cavity polaritons. For 225-fs pulses, shorter than the cavity Rabi cycle period of 1000 fs, this shift decouples excitons and cavity photons for the duration of the pulse, interrupting the periodic energy exchange between photonic and electronic states. For 1500-fs pulses, longer than the Rabi cycle period, however, the Stark shift does not affect the strong coupling. The two regimes are marked by distinctly different line shapes in ultrafast reflectivity measurements—regardless of the Stark field intensity. The crossover marks the transition from adiabatic to diabatic switching of strong light–matter coupling.

The achievement of strong coupling between light fields and matter excitations has marked a cornerstone of modern physics, both from a fundamental science viewpoint and for the implementation of new classical and quantum technologies. On the one hand, the ability to engineer repeated cycles of energy exchange between single atoms or atomic Bose–Einstein condensates (BEC) and photons confined in cavities, led to the development of a new research branch of cavity quantum electrodynamics, which allowed for implementation and testing of textbook Gedanken experiments [1, 2]. This progress is closely related to the emerging field of quantum information science, constituting the first test-bed for the implementation of secure quantum communication [3], quantum metrology [4] and future quantum computers [5]. On the other hand, the need for scalable platforms and room-temperature operation for technological applications inspired the investigation of strong coupling between light and solid-state systems like semiconductor quantum dots [6, 7], semiconductor quantum wells [8] and, more recently, organic [9] and two-dimensional materials [10]. Such solid-state systems also enable controlling the dynamics of strong coupling, which is challenging in atomic systems.

In semiconductor microcavities, strong light–matter coupling leads to the formation of cavity exciton–polaritons separated in frequency by twice the vacuum Rabi frequency Ω_R , with unique optical [11] and electronic properties [12]. Due to their mixed light–matter character which equips them with low masses and yet strong mutual interactions, polaritons have enabled the observation of high-temperature BEC [13–15], polariton lasing [16, 17], Bogoliubov excitations [18–20] and unconventional quantum fluidity [21–24]. Optical parametric oscillation in microcavities [25] enables generation of entangled photons from nanometer-scale devices [26]. Tunneling [27], switching [28, 29] and spin devices [30, 31] have evidenced the technological potential for high-frequency opto-electronic applications.

Dynamics of strongly coupled light–matter systems has attracted significant interest lately. A key factor for quantum information processing is to preserve coherence by non-invasive, reversible switching of light–matter coupling, as recently demonstrated using acoustic shockwaves [32], dc electrical modulation [33] and

photodoping [34]. However, these techniques are inherently limited to timescales slower than the Rabi cycle, by up to many orders of magnitude. Thus far, accessing femtosecond time scales has necessitated destroying or activating the strongly coupled state by, e.g., introducing charge carriers [35, 36]. Such invasive schemes alter the components of the light–matter coupled system for the duration of the carrier lifetime. In comparison, reversible modulation dynamics have thus far remained unexplored on time scales on the order of and shorter than the Rabi cycle time.

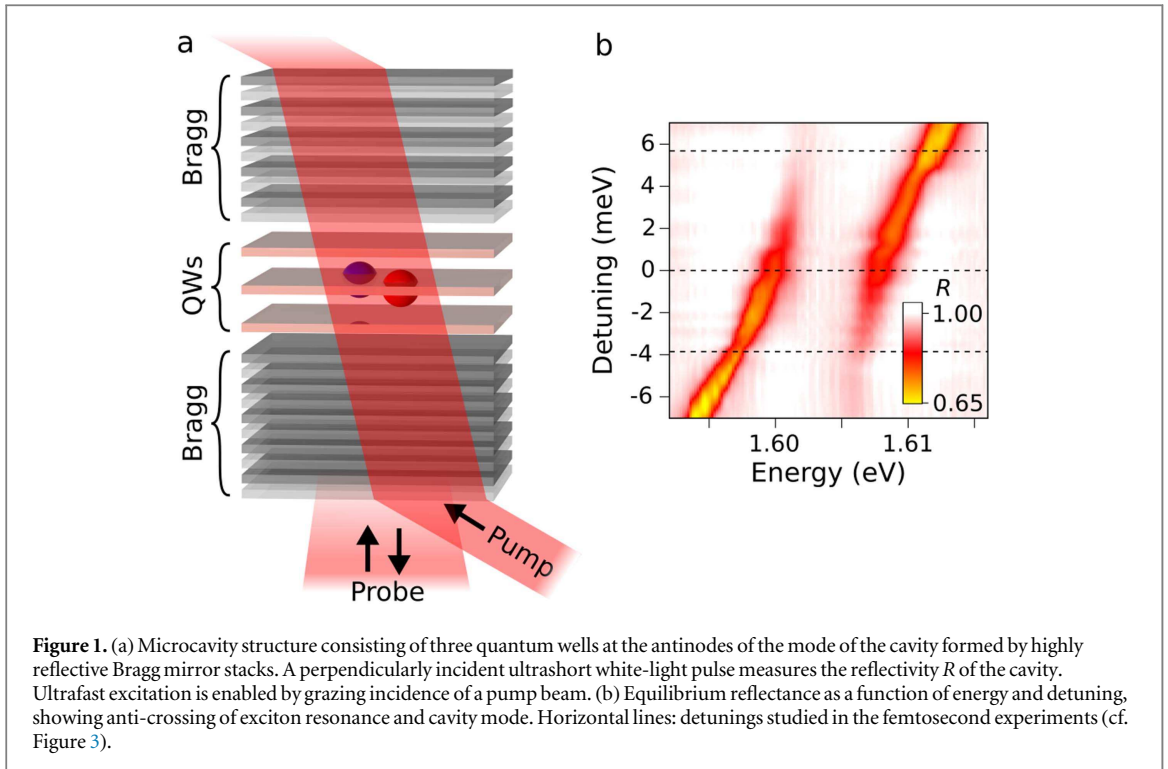
Here, we investigate noninvasively the ultrafast dynamics of cavity exciton–polaritons in a strongly coupled GaAs/AlGaAs microcavity, reversibly disrupting light–matter coupling on a time scale of the Rabi cycle period, $t_R = 2\pi/\Omega_R$. We demonstrate the crossover from quasi-equilibrium to diabatic dynamics of polaritons exposed to the ultrafast optical potential of a strong, red-detuned pump pulse of variable duration t_p , which noninvasively induces an instantaneous blue shift of the polariton doublet during its presence, through the ac Stark effect [37, 38]. Our approach enables ultrafast modulation on the femtosecond time scale and opens up a new regime of dynamics of strong coupling on timescales faster than the Rabi cycle of light–matter energy exchange, while the time scale of the dynamics is limited only by the pulse duration. With this unique capability we show two distinctly different regimes of noninvasive modulation, slower or faster than the light–matter energy exchange rate. For pump pulses shorter than t_R , we show that the cavity–exciton strong coupling is interrupted for the duration of the pulse, resulting in dynamical line broadening and a temporally discontinuous response observed in ultrafast reflection measurements. On the contrary, for pulses $t_p > t_R$, the Stark shift does not affect light–matter coupling, and the spectral signature of the polariton doublet remains intact apart from an adiabatic common-mode frequency shift. In both cases, these features are robust under variation of the pump intensity over more than one order of magnitude. In an intuitive picture, the two qualitatively different regimes are characterized as follows: for $t_p < t_R$, the Stark pulse induces a diabatic modulation of light–matter coupling, where the coupling strength is modified faster than a single cavity–exciton energy exchange. Here, cavity–exciton coupling does not govern the dynamics of light–matter interaction; instead, the Stark pulse couples mainly to the exciton leading to strong dynamical broadening, and the cavity passively modifies the spectral characteristics observed in reflectance due to its photonic density of states. Conversely, for $t_p > t_R$, exciton and light field exchange excitation more than once during t_p . Since the Stark pulse does not interrupt cavity–exciton coupling, polaritons remain the proper eigenstates of the system and retain their equilibrium linewidths during interaction with the pump field. Experimentally, the diabatic dynamics is very clearly observed on time scales of one fourth of the vacuum Rabi cycle (i.e., $t_p \approx t_R/4$). In fact, our calculations show that already for Stark pulses slightly shorter than $t_p \approx t_R/2$ the diabatic condition is approached.

Our microcavity structure, schematized in figure 1(a), consists of a $\lambda/2$ -thick AlAs layer embedded between two $\text{Ga}_{0.8}\text{Al}_{0.2}/\text{AlAs}$ distributed Bragg reflectors (DBR), with a total of 20 and 16 pairs for bottom and top reflector, respectively, resulting in a cavity Q -factor of $Q \sim 2400$. At each of the three antinodes of the resulting high-quality $3\lambda/2$ microcavity, single 6.5-nm-thick GaAs quantum wells (QWs) were grown. The Bragg structure is tapered along one in-plane axis, which allows for tuning the cavity mode at E_c with respect to the equilibrium exciton energy E_x^0 . In figure 1(b), the equilibrium reflectivity at a temperature of 4 K is plotted as a function of detuning for normal incidence, showing the expected anti-crossing behavior of cavity mode and excitonic resonance.

At zero detuning, lower (LP) and upper polariton (UP) are separated in energy by 8 meV, corresponding to $t_R = 2h/(E_{UP} - E_{LP}) \cong 1$ ps, where E_{LP} and E_{UP} denote the respective polariton energies.

In our experiment, we measure the ultrafast modulation of the reflectivity R of the strongly coupled structure after excitation with pump pulses centered at 1.55 eV, red-detuned relative to E_x^0 by ~ 55 meV, using femtosecond white-light supercontinuum pulses generated in a sapphire crystal (in a similar setup to that of [37]). The reflectivity spectra are normalized to the spectrum of the white light probe pulse reflected from a metallic mirror without spectral features in the region of interest. The pump beam is kept at a power level at which no significant carrier generation through, e.g., multi-photon processes occurs. Both, pump and probe are derived from a 250-kHz regenerative amplifier with transform-limited 225-fs pulses. The sample is kept at 4 K in a cryostat at all times.

In the first set of experiments, we modulated the exciton–polariton energy levels by the Stark pulse in an adiabatic regime—with a pulse duration longer than the Rabi oscillation period, $t_p > t_R$. Pump pulses of 1500 fs duration (ps-excitation) were obtained by stretching the 225-fs pulses of the laser source using a grating stretcher. The peak intensity was kept at 3.2 GW cm^{-2} , while various detunings $\Delta E = E_c - E_x^0$ were selected. The instantaneous absolute reflectivity R of our microcavity, plotted in figure 2(a) for $\Delta E = 0$ as a function of energy and delay time τ between pump and probe pulses, demonstrates that the Stark shift adiabatically sets in and persists for the duration of the pump pulse, without signatures of perturbed free induction decay [39]. Moreover, since the perturbation lasts longer than the Rabi cycle time, the reflectivity in the spectral range between LP and UP remains unchanged, and their dynamics can be observed individually as a slight shift of the respective minima of the reflectivity towards higher energies, with no spectral overlap between LP and UP.



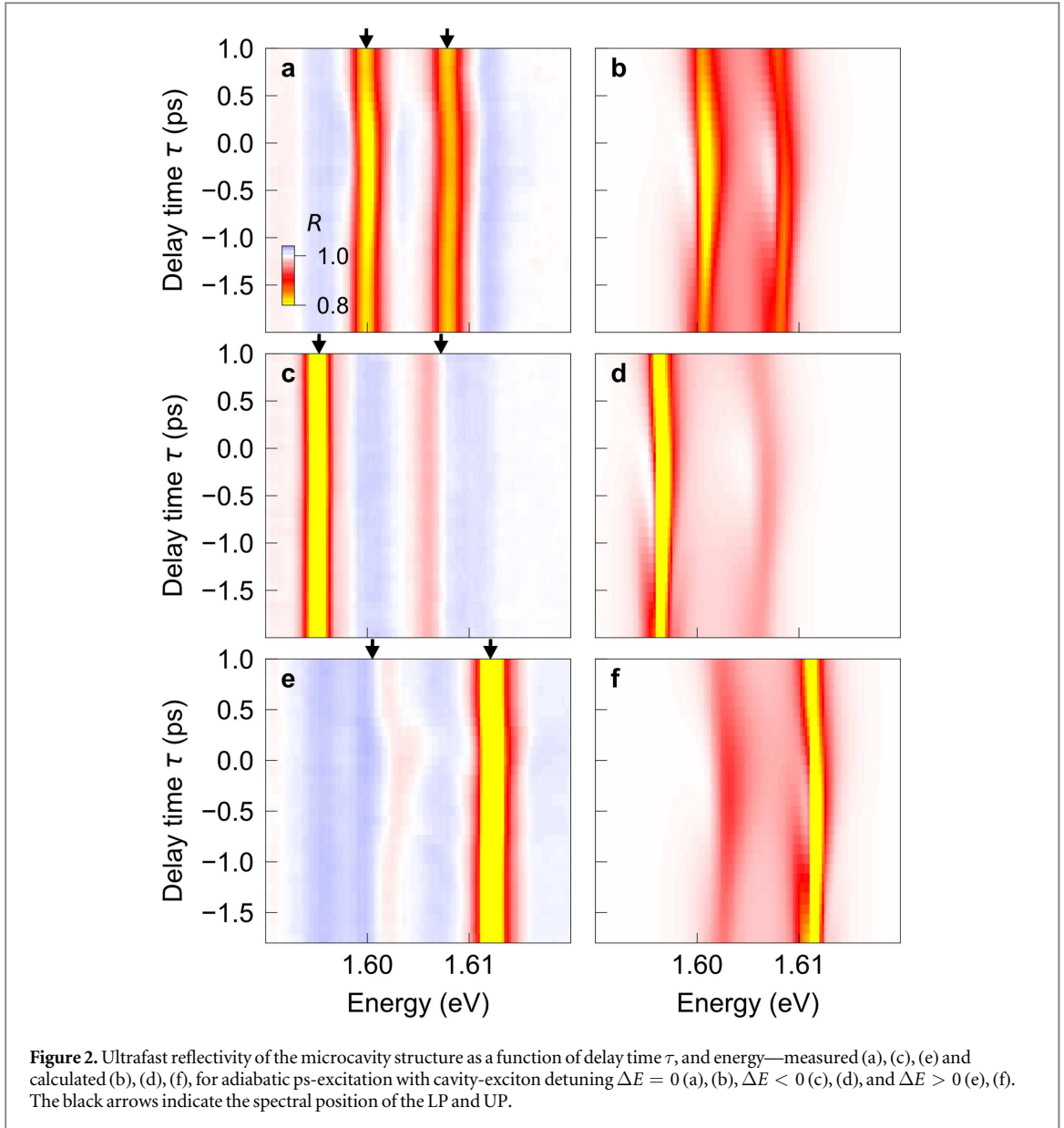
After time-zero, the reflectivity spectrum recovers completely, evidencing that no significant amount of carriers are generated during excitation. Our theoretical analysis detailed further below fully supports this result (figure 2(b)). The response remains qualitatively similar for detunings $\Delta E \neq 0$ (figures 2(c) and (e)), yet, changing the detuning ΔE allows for tuning the Hopfield coefficients for the two polariton branches, and thus their composition. While $\Delta E = 0$ yields that both polariton branches consist of equal fractions of excitonic and light field components, $\Delta E < 0$ yields a more photonic LP and a more excitonic UP, and vice versa. In each case, the more excitonic polariton exhibits the stronger response.

A fundamentally different behavior is observed by using ultrashort 225-fs pulses (fs-excitation) [37], where peak pulse intensities equivalent to the ps-case were chosen to obtain an instantaneous ac Stark shift of the same magnitude, for comparability. In this setting, a qualitatively different spectral shape is observed. In figure 3, we plot the corresponding reflectivity spectra analogously to figure 2. Before time-zero, perturbed free induction decay of the coherent polarization of the probe pulse leads to spectral and temporal oscillations of the reflectivity, exhibiting interference between the two polariton branches. As time zero is approached, these oscillations diverge in wavelength and finally transition into the doubly-dispersive signature caused by the ac Stark shift of the polariton doublet [37]. In this setting of $t_p < t_R$, the spectral width of this feature exceeds the polariton Rabi splitting, and a continuous spectral line shape extending beyond both polariton branches results. For zero detuning (figure 3(a)) both polariton branches completely collapse at $\tau = -200$ fs, and a single, broadband signature emerges, which represents the response of the uncoupled exciton.

These dynamics are strongest at slightly negative delay times owed to the delayed buildup of polarization in the structure, leading to maximum interaction between pump and probe pulses for probe pulses slightly preceding the pump pulse. Our theoretical model, detailed further below, fully reproduces the spectral signatures including coherent oscillations as well as the twinned polariton signature near time zero (figure 3), and allows us to determine the polariton decoherence time of $T_2 \cong 1$ ps.

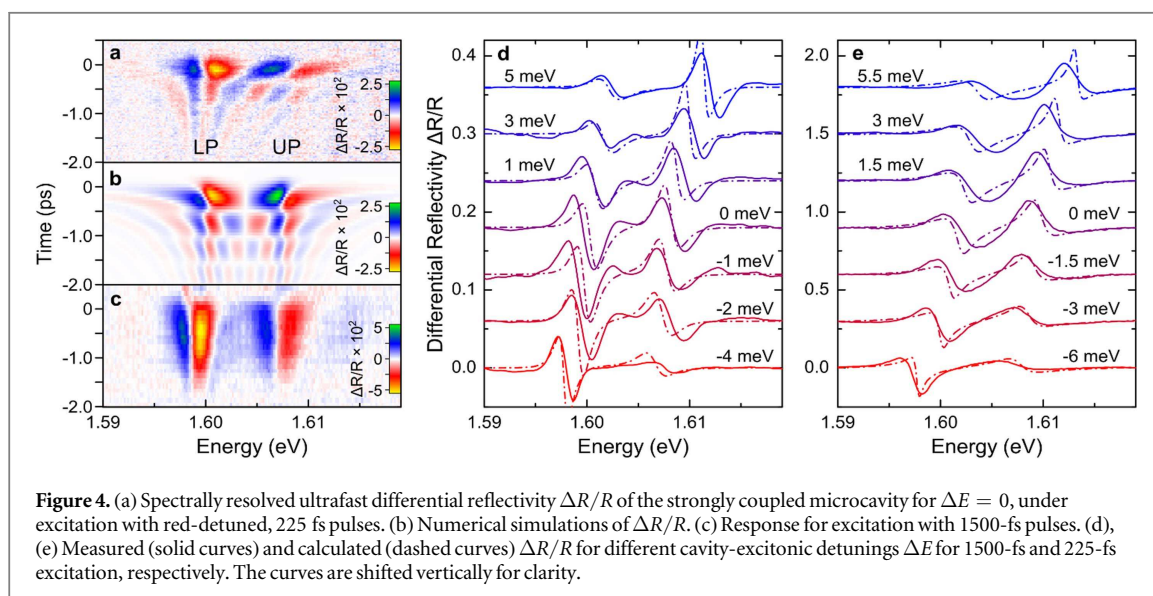
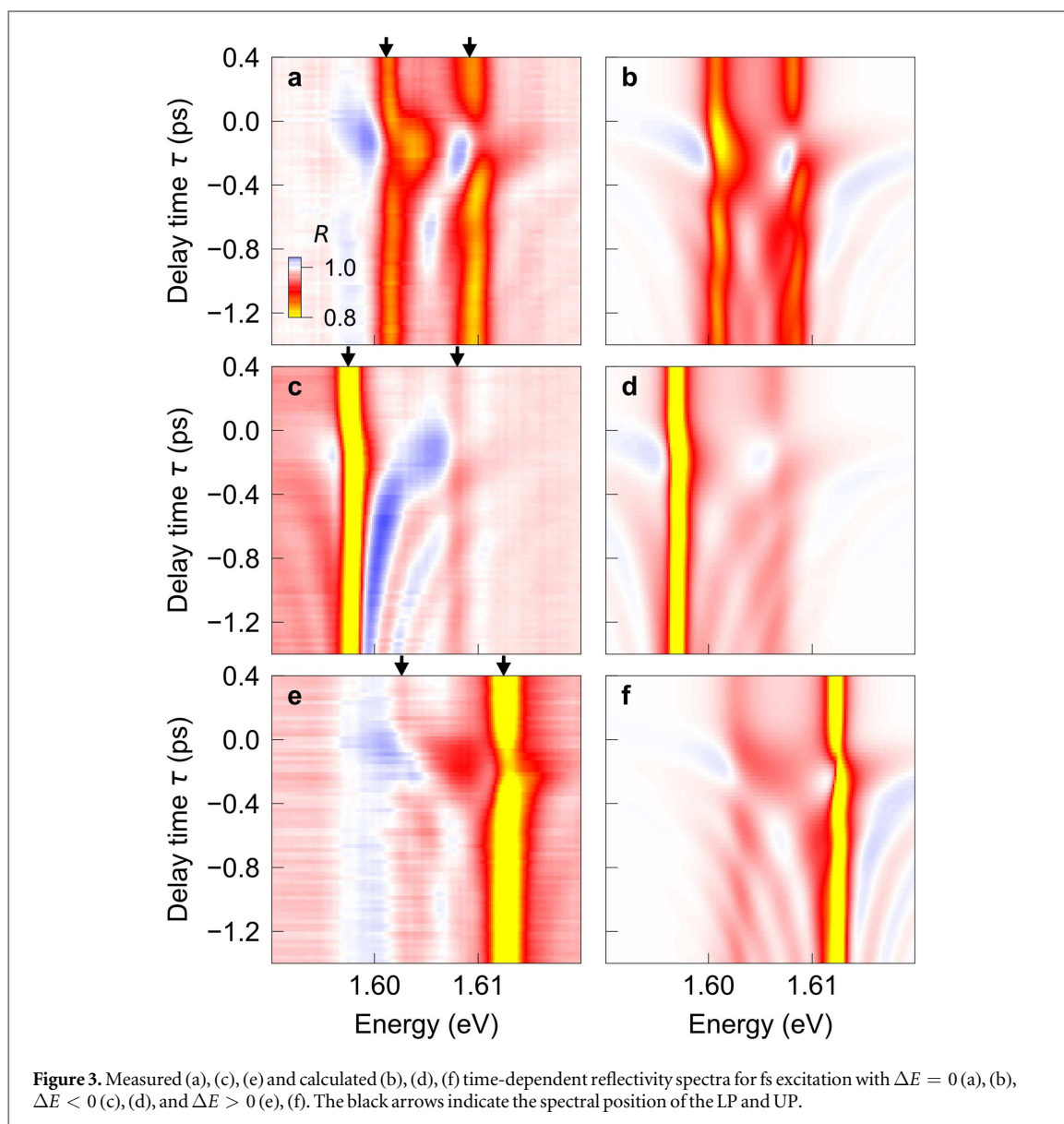
We show that similar to the ps case, the polariton branch with the larger exciton fraction interacts more strongly with the pump pulse and hence, for fs excitation, displays strong spectral broadening, while the other branch exhibits a more narrowband response—with good agreement to the calculated response (figure 3).

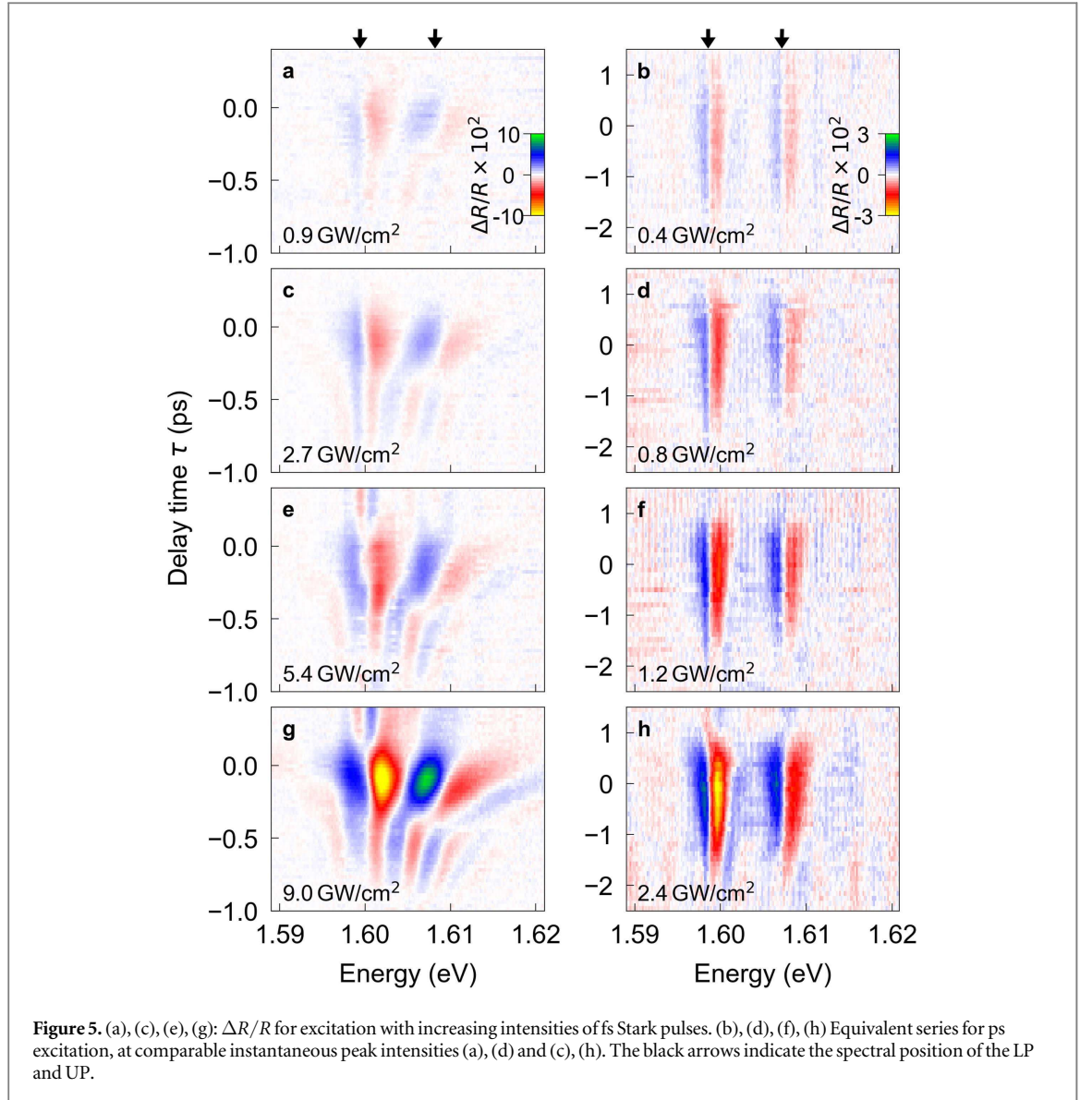
Next, in order to better understand the effect of the diabatic driving of the excitonic resonance we measure the differential reflectivity $\Delta R/R$ as a function of delay for fs (figure 4(a); theory: figure 4(b)) and ps excitation (figure 4(c)), and compare it at a fixed delay slightly before time-zero where the largest signal is attained, for different values of the detuning ΔE (figures 4(d) and (e), solid lines). At $\Delta E = 0$, the separated (d) or merged (e) character of the polariton doublet, respectively, in these two regimes is clearly observed analogously to figures 2 and 3. For ps excitation (d), the spectral widths of the signatures of LP and UP are almost identical even for nonzero values of ΔE . In this case, the equilibrium linewidth remains the dominant contribution, and only little additional broadening is introduced by the dynamic ac Stark shift. Note that the amplitude of each feature in



$\Delta R/R$ varies according to its spectral distance from the cavity line. For fs excitation (e), however, the dynamical broadening dominates. At $\Delta E = -6$ meV, the specific Hopfield coefficients render the LP strongly photon-like. Since the cavity resonance is not affected by the Stark effect, the LP line width is thus close to the equilibrium linewidth. In contrast, the more exciton-like UP is fully affected by the ac Stark shift and exhibits a spectral shape significantly broader than in the equilibrium situation. As $\Delta E = 0$ is approached, the excitonic fraction is more evenly distributed and the line widths of LP and UP become comparable. Finally, for $\Delta E > 0$, they cross over such that at +5.5 meV, we observe a broadband LP and a narrowband UP resonance.

In order to rule out nonlinear optical or carrier-related effects as the origin of the polariton broadening, we systematically vary the pump intensity in both the fs and the ps case over approximately one order of magnitude, as plotted in figures 5(a), (c), (e), (g) and (b), (d), (f), (h), respectively. For better comparability, we again chose higher pump powers in the ps case, resulting in similar instantaneous Stark shifts in the panel pairs (a), (d), and (c), (h). Furthermore, we again restrict the pump power to levels at which no significant carrier generation by two-photon absorption (TPA) of the Stark pulse occurs. For our highest pump intensities of 9 GW cm^{-2} and 225 fs pulses (2.4 GW cm^{-2} , 1500-fs pulses), we estimate by the TPA coefficient of GaAs of $\sim 20 \text{ cm GW}^{-1}$ [40] that our strongest pulses inject a sheet carrier density of $4.8 \times 10^{11} \text{ cm}^{-2}$ ($2.2 \times 10^{11} \text{ cm}^{-2}$) per QW, which should not result in strong carrier-related signatures in $\Delta R/R$. This estimate is confirmed by the small residual differential reflectivity signal at positive delay times serving as an experimental probe for renormalization effects, which are smaller than the Stark-induced signal near time-zero by approximately an order of magnitude or more, in every case (e.g., panel (g) for $\tau = 0.4$ ps). We find that the spectro-temporal signature is independent of pump power up to a scale factor in $\Delta R/R$ within each power series, yet it fundamentally differs between ps and fs





cases. We additionally point out that the grating configuration used to obtain the ps pump pulses leaves their time-integrated spectral shape identical to the fs case. Hence, ruling out nonlinearities related to instantaneous pump intensity and possible spectral effects, we conclude that the duration of the pump pulse alone is responsible for the characteristic line shape of $\Delta R/R$.

Our theoretical modeling of the observed dynamics is based on an input–output single-particle mean-field approach [41, 42], incorporating the coupling of excitonic and photonic modes ψ_x and ψ_c via the Rabi frequency Ω_R (taken equal to 8 meV for the calculations):

$$i\hbar\partial_t \begin{pmatrix} \psi_x \\ \psi_c \end{pmatrix} = \begin{pmatrix} 0 \\ \sqrt{\kappa_1} F(t) \end{pmatrix} + \begin{pmatrix} E_x(t) - i\hbar\kappa_x/2 & \hbar\Omega_R/2 \\ \hbar\Omega_R/2 & E_c - i\hbar\kappa_c/2 \end{pmatrix} \begin{pmatrix} \psi_x \\ \psi_c \end{pmatrix}, \quad (1)$$

$$E_x(t) = E_x^0 + f_p e^{-t^2/2\sigma_p^2}, \quad (2)$$

$$F(t) = f_{pb} e^{i\omega_{pb}t} e^{-(t-t_{pb})^2/2\sigma_{pb}^2}, \quad (3)$$

$$\kappa_c = \kappa_1 + \kappa_2. \quad (4)$$

Here, $E_x(t)$ is the exciton energy including the instantaneous ac Stark shift, modeled with a Gaussian temporal profile of amplitude f_p and duration σ_p chosen to represent Stark pulses with full width half maximum of either 225 fs or 1500 fs, $\hbar\kappa_x = 4.25$ meV is the exciton non-radiative decay rate, and κ_c is the combined loss rate constituting of the loss rates of the front and back DBR, $\hbar\kappa_1 = 0.1$ meV and $\hbar\kappa_2 = 0.16$ meV. The probe pulse is modeled by $F(t)$ with a Gaussian profile, amplitude f_{pb} and duration σ_{pb} chosen for a pulse of FWHM of 250 fs.

Our theory fully reproduces the spectro-temporal signature of the dynamic Stark shift, including the perturbed free induction decay at negative delay times with interference features of both polariton branches (see figures 2 and 3). Spectra extracted near time-zero are plotted in figures 4(d) and (e) as dashed lines along the corresponding experimental data. Both, the spectral shape and the relative reflection amplitudes of the LP and UP are rendered correctly under ps as well as fs excitation. The theory confirms the plateau-shaped spectral range of vanishing $\Delta R/R$ signal between the individual Stark shift signatures of LP and UP shown in figure 4(d). Likewise, the merged spectral signature of both polaritons under fs excitation is rendered (figure 4(e)). Our calculations thus confirm the qualitatively different scenarios for $t_p < t_R$ and $t_p > t_R$, corresponding to the large spectral broadening of a polariton doublet with frozen exciton-cavity exchange, or adiabatic perturbation, respectively (see supplementary material available online at stacks.iop.org/NJP/20/013032/mmedia for detailed calculation results).

In conclusion, we have demonstrated the crossover from adiabatic to diabatic perturbation of a strongly coupled exciton–polariton microcavity excited with red-detuned, intense pump pulses longer or shorter in duration than the Rabi cycle, respectively. Strongly increased broadening exceeding the vacuum Rabi splitting, and ultrafast collapse and revival of the polariton doublet results for sub-Rabi-cycle excitation, demonstrating that the limit of a frozen polariton is approached, where no exchange between exciton and light field takes place during the perturbation. Adiabatic perturbation at identical pump peak intensities, on the contrary, leads to a collective shift of the polariton doublet. Tuning the cavity relative to the resonance enabled us to distribute the ac Stark shift by modifying the excitonic and photonic fraction of the polaritons. Our theory reproduces the line shape quantitatively. The crossover between adiabatic and diabatic control of light–matter coupling demonstrated here paves the way for fundamental research and practical applications in the study of strongly-coupled systems and novel quantum technologies.

Acknowledgments

This work has been partially supported by the National Science Foundation under grant DMR-1104383 and PHY-1205762. The work at Princeton was partially funded by the Gordon and Betty Moore Foundation as well as the National Science Foundation MRSEC Program through the Princeton Center for Complex Materials (DMR-0819860). CL acknowledges support by the Alexander von Humboldt Foundation.

References

- [1] Haroche S 2013 Nobel lecture: controlling photons in a box and exploring the quantum to classical boundary *Rev. Mod. Phys.* **85** 1083
- [2] Brenneke F, Donner T, Ritter S, Bourdel T, Köhl M and Esslinger T 2007 Cavity QED with a Bose–Einstein condensate *Nature* **450** 268–71
- [3] Gisin N, Ribordy G, Tittel W and Zbinden H 2002 Quantum cryptography *Rev. Mod. Phys.* **74** 145
- [4] Giovannetti V, Lloyd S and Maccone L 2011 Advances in quantum metrology *Nat. Photon.* **5** 222
- [5] Ladd T D, Jelezko F, Laflamme R, Nakamura Y, Monroe C and O’Brien J L 2010 Quantum Computers *Nature* **464** 45
- [6] Reithmaier J P, Sek G, Löffler A, Hofmann C, Kuhn S, Reitzenstein S, Keldysh L V, Kulakovskii V D, Reinecke T L and Forchel A 2004 Strong coupling in a single quantum dot–semiconductor microcavity system *Nature* **432** 197
- [7] Hennessy K, Badolato A, Winger M, Gerace D, Atatüre M, Gulde S, Fält S, Hu E L and Imamoglu A 2007 Quantum nature of a strongly coupled single quantum dot–cavity system *Nature* **445** 896
- [8] Weisbuch C, Nishioka M, Ishikawa A and Arakawa Y 1992 Observation of the coupled exciton-photon mode splitting in a semiconductor quantum microcavity *Phys. Rev. Lett.* **69** 3314
- [9] Daskalakis K S, Maier S A and Kéna-Cohen S 2015 Spatial coherence and stability in a disordered organic polariton condensate *Phys. Rev. Lett.* **115** 035301
- [10] Lundt N et al 2016 Room-temperature Tamm-plasmon exciton–polaritons with a WSe₂ monolayer *Nat. Commun.* **7** 13328
- [11] Aßmann M, Veit F, Bayer M, van der Poel M and Hvam J M 2009 Higher-order photon bunching in a semiconductor microcavity *Science* **325** 297
- [12] Schneider C et al 2013 An electrically pumped polariton laser *Nature* **497** 348–52
- [13] Deng H, Weihs G, Santori C, Bloch J and Yamamoto Y 2002 Condensation of semiconductor microcavity exciton polaritons *Science* **298** 199
- [14] Kasprzak J et al 2006 Bose–Einstein condensation of exciton polaritons *Nature* **443** 409
- [15] Balili R, Hartwell V, Snoke D, Pfeiffer L and West K 2007 Bose–Einstein condensation of microcavity polaritons in a trap *Science* **316** 1007
- [16] Tempel J-S, Veit F, Aßmann M, Kreilkamp L E, Höfling S, Kamp M, Forchel A and Bayer M 2012 Temperature dependence of pulsed polariton lasing in a GaAs microcavity *New J. Phys.* **14** 083014
- [17] Deng H, Weihs G, Snoke D, Bloch J and Yamamoto Y 2003 Polariton lasing versus photon lasing in a semiconductor microcavity *Proc. Natl Acad. Sci.* **100** 15318
- [18] Utsunomiya S et al 2008 Observation of Bogoliubov excitations in exciton–polariton condensates *Nat. Phys.* **4** 700
- [19] Kohnle V, Léger Y, Wouters M, Richard M, Portella-Oberli M T and Deveaud-Plédran B 2011 From single particle to superfluid excitations in a dissipative polariton gas *Phys. Rev. Lett.* **106** 255302
- [20] Pieczarka M et al 2015 Ghost branch photoluminescence from a polariton fluid under nonresonant excitation *Phys. Rev. Lett.* **115** 186401
- [21] Amo A et al 2011 Polariton superfluids reveal quantum hydrodynamic solitons *Science* **332** 1167

- [22] Aßmann M, Tempel J-S, Veit F, Bayer M, Rahimi-Iman A, Löffler A, Höfling S, Reitzenstein S, Worschech L and Forchel A 2011 From polariton condensates to highly photonic quantum degenerate states of bosonic matter *Proc. Natl Acad. Sci.* **108** 1804
- [23] Amo A, Lefrère J, Pigeon S, Adrados C, Ciuti C, Carusotto I, Houdré R, Giacobino E and Bramati A 2009 Superfluidity of polaritons in semiconductor microcavities *Nat. Phys.* **5** 805
- [24] Amo A et al 2009 Collective fluid dynamics of a polariton condensate in a semiconductor microcavity *Nature* **457** 291
- [25] Saba M et al 2001 High-temperature ultrafast polariton parametric amplification in semiconductor microcavities *Nature* **414** 731
- [26] Einkemmer L, Vörös Z, Weihs G and Portolan S 2015 Polarization entanglement generation in microcavity polariton devices *Phys. Status Solidi b* **252** 1749
- [27] Nguyen H S et al 2013 Realization of a double-barrier resonant tunneling diode for cavity polaritons *Phys. Rev. Lett.* **110** 236601
- [28] De Giorgi M et al 2012 Control and ultrafast dynamics of a two-fluid polariton switch *Phys. Rev. Lett.* **109** 266407
- Cancellieri E, Marchetti F M, Szymanska M H and Tejedor C 2011 Multistability of a two-component exciton–polariton fluid *Phys. Rev. B* **83** 214507
- [29] Ballarini D, De Giorgi M, Cancellieri E, Houdré R, Giacobino E, Cingolani R, Bramati A, Gigli G and Sanvitto D 2013 All-optical polariton transistor *Nat. Commun.* **4** 1778
- [30] Amo A, Liew T C H, Adrados C, Houdré R, Giacobino E, Kavokin A V and Bramati A 2010 Exciton–polariton spin switches *Nat. Photon.* **4** 361
- [31] Adrados C, Liew T C H, Amo A, Martín M D, Sanvitto D, Antón C, Giacobino E, Kavokin A, Bramati A and Viña L 2011 Motion of spin polariton bullets in semiconductor microcavities *Phys. Rev. Lett.* **107** 146402
- [32] Berstermann T, Brüggemann C, Akimov A V, Bombeck M, Yakovlev D R, Gippius N A, Scherbakov A V, Sagnes I, Bloch J and Bayer M 2012 Destruction and recurrence of excitons by acoustic shock waves on picosecond time scales *Phys. Rev. B* **86** 195306
- [33] Anappara A A and Tredicucci A O 2005 Electrical control of polariton coupling in intersubband microcavities *Appl. Phys. Lett.* **87** 051105
- [34] Schwartz T, Hutchison J A, Genet C and Ebbesen T W 2011 Reversible switching of ultrastrong light–molecule coupling *Phys. Rev. Lett.* **106** 196405
- [35] Günter G et al 2009 Sub-cycle switch-on of ultrastrong light–matter interaction *Nature* **458** 178
- [36] Porer M, Ménard J-M, Leitenstorfer A, Huber R, Degl’Innocenti R, Zanotto S, Biasiol G, Sorba L and Tredicucci A 2012 Nonadiabatic switching of a photonic band structure: ultrastrong light–matter coupling and slow-down of light *Phys. Rev. B* **85** 081302(R)
- [37] Hayat A, Lange C, Rozema L A, Darabi A, van Driel H M, Steinberg A M, Nelsen B, Snoke D W, Pfeiffer L N and West K W 2012 Dynamic Stark effect in strongly coupled microcavity exciton–polaritons *Phys. Rev. Lett.* **109** 033605
- [38] Cancellieri E, Hayat A, Steinberg A M, Giacobino E and Bramati A 2014 Ultra-fast Stark-induced polaritonic switches *Phys. Rev. Lett.* **112** 053601
- [39] Sokoloff J P, Joffre M, Fluegel B, Hulin D, Lindberg M, Koch S W, Migus A, Antonetti A and Peyghambarian N 1988 Transient oscillations in the vicinity of excitons and in the band of semiconductors *Phys. Rev. B* **38** 7615
- [40] Van Stryland E W, Woodall M A, Vanherzeele H and Soileau M 1985 Energy band-gap dependence of two-photon absorption *Opt. Lett.* **10** 490
- [41] Karr P, Baas A and Giacobino E 2004 Twin polaritons in semiconductor microcavities *Phys. Rev. A* **69** 063807
- [42] Walls D F and Milburn G J 2008 *Quantum Optics* (Berlin: Springer)